

MOLECULAR-BEAM STUDIES OF CARBONACEOUS CLUSTERS*

Thomas J. Butenhoff and Eric A. Rohlfing
Combustion Research Facility
Sandia National Laboratories
Livermore, CA 94551

Keywords: Carbon and carbonaceous clusters, soot formation.

INTRODUCTION

Carbon clusters ranging in size from a few to a few hundred atoms are currently a topic of intense theoretical and experimental study. Recent advances have made it possible to synthesize C_{60} , buckminsterfullerene, and other even-numbered carbon clusters ("fullerenes") in macroscopic quantities so that these spherical clusters, and their chemical derivatives, have made the leap from laboratory curiosities to potentially important materials. This has led to an explosion of research in fullerene characterization and chemistry. Fullerenes are ubiquitous to a variety of growth environments that abound in species with elements other than carbon and are implicated in environments ranging from sooting flames to interstellar space. Fullerene ions can be observed as the dominant mass spectral features when a variety of substrates, including polycyclic aromatics,¹ polymers,² and soot particles,³ are vaporized by a laser *in vacuo*. They are also observed in sooting flames in the region where soot particles first form.^{4,5}

No matter what the conditions of growth, it now seems clear that the fullerenes and carbon (or soot) particles are intimately connected. At question is the model for particle growth proposed by Kroto^{6,7} and Smalley⁸ that has been postulated to account for the molecular beam results and has been extended to explain soot formation in combustion. Simply put, this model assumes that the nucleus of the growing particle is an incomplete spherical shell that accumulates primarily graphitic carbon on its reactive edges. A fullerene is formed in the rare event that a shell closes, thereby becoming inert with respect to further growth. This model has been the subject of much debate⁹ between its proponents and those who favor the more traditional mechanism for soot formation. The traditional view¹⁰⁻¹² explains the rapid growth of soot at its inception by reactions between large polycyclic aromatics that are found in abundance in sooting flames. Subsequent addition of mass then proceeds via surface growth reactions between the soot particle and smaller gas phase reactants. The observation of fullerenes in sooting flames by Homann et al.^{4,5} has been taken by some as evidence for the spiraling shell model. However, Homann et al. interpret their results within the traditional mechanism and hypothesize that the fullerenes are formed from nascent soot particles by an evaporative process.

We have begun a program to study the reactions of large carbon clusters and their hydrogenated analogs, which we shall call carbonaceous clusters, and attempt to make the connection between the molecular beam/flow reactor environment and a sooting flame. Smalley and co-workers have previously examined the reactivities of small ($n < 20$) and large ($n > 40$) carbon clusters in molecular beam work with the laser vaporization clusters source. In one study, Heath et al.¹³ looked at the C_n and C_nH_m ions produced by the multiphoton ionization of neutrals created by the addition of various hydrogen-containing reactants to the carrier gas upstream of the laser-induced plasma. In another study, Zhang et al.⁸ examined the reactivities of the large neutral clusters in a fast flow reactor located downstream of the vaporization region; they used single-photon ionization to probe the neutral cluster distributions. These experiments showed the unique inertness of the fullerenes to chemical attack by a variety of reactants. In both these studies, the authors used a linear time-of-flight mass spectrometer (TOF MS) with moderate mass resolution. In particular, the mass resolution in the fullerene study was insufficient to observe the products of the facile reactions between the injected reactant and the

* This work supported by the United States Department of Energy, Office of Basic Energy Sciences, Chemical Sciences Division.

odd-numbered clusters (which cannot achieve closed shells). These products appeared as an unresolved background from which the fullerene peaks stood out.

In this paper, we summarize results from experiments in which the formation of clusters is modified by addition of hydrogen to the carrier gas that flows over the graphite in the laser-vaporization source.¹⁴ The resulting carbon and carbonaceous clusters (for $n \geq 20$) are gently single-photon ionized by a vacuum ultraviolet laser (F_2 158 nm) in order to probe the neutral cluster distribution without extensive perturbation from ionization efficiency or multiphoton fragmentation. The cluster ions are subsequently mass analyzed in a high resolution reflectron TOF MS. The resolution of this instrument at high mass ($M/\Delta M \sim 1700$ at 720 amu) allows us to completely resolve mass peaks separated by 1 amu, i.e. each value of m in C_nH_m . By adjusting the growth conditions in the cluster source through combinations of carrier gas density and residence times, we can produce carbon cluster distributions that exhibit wide variations in their degree of local maxima, or magic numbers. For example, we find low-growth conditions in which the abundances of odd clusters are nearly equal to those of the fullerenes. Alternatively, we can create very "magic" distributions in which the fullerenes, especially C_{60} , dominate the neighboring odd clusters. The carbonaceous cluster distributions produced by the addition of hydrogen to the carrier gas always show a dramatic preference for the formation of C_nH_m clusters with odd n . Remarkably, the clusters with even n appear predominantly as pure C_n , i.e. the fullerenes. We quantify these qualitative trends through a hydrogenation analysis that determines the fraction of each cluster that is hydrogenated and the distribution of hydrogens among the C_nH_m . The quantitative results (hydrogenation fraction, hydrogenation distribution, C/H ratio, etc.) show vivid evidence for the formation of long polyacetylenes, C_nH_2 , for even n up to $n=44$. In addition, they reveal a dramatic change in hydrogenation behavior at about $n=40$ that provides more indirect evidence in support of the fullerene structural hypothesis. Finally, we discuss the implications of our results with respect to incomplete spherical shells and the corresponding model for particle growth.

EXPERIMENTAL TECHNIQUE

Carbon clusters are created by laser vaporization of graphite (3.2-mm-diameter rod, Pure Tech, 99.99%) into the helium flow following a piezoelectrically actuated pulsed valve that operates with 10-100 psig backing pressure and a 1-mm-diameter orifice. The vaporization laser is the second harmonic of a Nd:YAG laser (Spectra Physics DCR-11) at 532 nm with a pulse length of 6-7 ns and energy of 17 mJ. The flow channel is 2.5 mm in diameter at the target rod and for 22 mm downstream; the last 12 mm of the channel forms a 30° conical nozzle from which the flow expands into a vacuum chamber pumped by an unbaffled diffusion pump (Varian VHS-10). The cluster/helium expansion is skimmed once in the source chamber (5-mm-diameter skimmer, Beam Dynamics) at 35 cm downstream of the source. The resulting molecular beam enters a second vacuum chamber pumped by a 500 l/s turbomolecular pump (Balzers TPU 510) and is further collimated by a second 5-mm skimmer (98 cm downstream) before entering the ionization chamber of the reflectron TOF MS, which is located 109 cm downstream of the source. Carbonaceous clusters, of the generic formula C_nH_m , are formed in the same manner as C_n except that the helium carrier gas is replaced by a mixture of H_2 in helium. Vacuum ultraviolet photoionization using the light from an excimer laser (Questek 2820) operated on the F_2 line at 158 nm (7.89 eV) creates cluster ions in the ion source of the reflectron TOF MS. Typical laser pulse length and fluence are ~ 17 ns and 0.1 mJ/cm², respectively. The timing for these experiments is controlled by two digital delay generators (SRS DG535) under computer control.

The reflectron TOF MS is a modified version of a commercially available instrument (R. M. Jordan Co.) and is arranged such that the initial ion-beam axis is collinear with the neutral cluster beam. The repeller-extractor and extractor-ground plate spacings are 1.9 cm and 0.95 cm, respectively; the repeller and extractor voltages are 1800 V and 1000 V, respectively. The ion beam (nominal energy 1400 eV) is accelerated out of the ionization source along the neutral beam for 0.5 cm before entering a static deflection field of 37 V/cm that extends for 3.8 cm. This field deflects the ions over a total angle of 7.2°. After passing the first flight region (97.7 cm), the ions are decelerated and re-accelerated in a two-stage reflector. The first stage is defined by two gridded plates separated by 1.2 cm and has a 1000 V potential increase. The second stage is

9.7 cm long and consists of 11 guard rings with elliptical openings terminated by the reflector plate. Final temporal focusing of the ions is achieved by fine adjustments of the electric field in the second stage by changing the voltage applied to the reflector plate (nominally 1620 V). Ions emerging from the reflector traverse the second field-free flight region of 64.2 cm in length before striking a 40-mm-diameter dual microchannel plate detector (R. M. Jordan Co.). The ion time-of-flight signals are amplified (Comlinear CLC 100) and digitized by a 400 MHz digital oscilloscope (LeCroy 9450). The TOF mass spectrum is acquired as separate summation averages (typically 1000 laser shots) in 50- μ s increments and is transferred from the digital oscilloscope to a host computer for analysis.

RESULTS

A. Mass Spectra

In Fig. 1 we display an example of the TOF mass spectrum of C_nH_m ions for $n=16-160$ obtained under moderate-growth source conditions with a 0.5% H_2/He mixture. We have taken many other C_n and C_nH_m mass spectra under low-growth and high-growth source conditions.¹⁴ Our definitions of the growth characteristics in the cluster source are predicated on the nature of the carbon-cluster mass spectrum taken under identical detection conditions. We define "low-growth" conditions as those under which the odd-numbered C_n are roughly as abundant as the even-numbered clusters in the region near $n=60$. A distribution near $n=60$ in which the even clusters, and particularly C_{60} , have considerably more intensity than the odd clusters defines "moderate growth" (see Fig. 1). For our cluster source with the flow channel described above, moderate growth is the norm, i.e. 100 psig backing pressure, full driving voltage applied to the valve, and vaporization timed to occur in the center of the gas pulse. Low growth can be achieved in several different ways: lowering the backing pressure to 10 psig, lowering the driving voltage on the piezoelectric valve, or by firing the vaporization laser early in the gas pulse. All of these approaches lower the effective density of the carrier gas over the target when the vaporization laser fires. We can also achieve high-growth conditions, in which C_{60} completely dominates the C_n distribution at $50 \leq n \leq 70$, by running under nominal conditions and increasing the length of the flow channel by 27 mm. The observation of enhanced even/odd alternation with increasing carrier gas in the source is consistent with the model proposed by Smalley and Kroto in which the fullerenes are the survivors of the cluster-growth process that ultimately leads to carbon particles. Increasing the carrier gas density provides greater containment of the carbon vapor in the laser-induced plasma and thus provides a higher density of growth species and leads to more rapid condensation.

The moderate-growth mass spectrum produced with a 0.5% H_2/He mixture in Fig. 1 shows hydrogenated clusters, C_nH_m , that appear both with n even and odd up to about $n=40$. At this point the odd clusters continue to appear predominantly as hydrogenated species while substantial intensities of even C_n appear above this hydrocarbon "soup". Figure 2 displays the comparison of the C_n and C_nH_m moderate-growth mass spectra for $n=21-24$ and $n=58-62$. For a given n , the signal for each mass peak in the C_nH_m spectrum has contributions from the ^{13}C isotopic variants of C_n and from the C_nH_m species and their ^{13}C isotopic variants. This convolution, which increases in severity with increasing n because the ^{13}C distribution widens, makes it impossible to determine the distribution of hydrogenated species directly from the mass spectrum. Note the propensity for the formation of C_nH_2 for the even-numbered clusters in the $n=21-24$ range. The C_nH_m spectrum for $n=58-62$ in Fig. 2 shows hydrogenation of both even and odd clusters near $n=60$. However, the extent of the hydrogenation is clearly much greater for the odd clusters; substantial amounts of the even clusters appear as bare carbon clusters. In the low growth case, the addition of hydrogen enhances the appearance of the even C_n , and especially C_{60} , with respect to the hydrocarbon background. Remarkably, this occurs even when the even clusters do not appear as "special" in the corresponding C_n spectrum.

B. Hydrogenation Analysis

To quantify the extent of hydrogenation and the distribution of hydrogen atoms for C_nH_m at a given n , we have developed a procedure in which the effects of the ^{13}C isotopic distribution are deconvoluted from the hydrogenation distribution. Ref. 14 describes this procedure in detail.

It is applicable to situations in which the hydrogenation distribution for cluster n ends before the one for cluster $n+1$ begins, i.e. $m \leq 11$. For the data presented here, we can apply the deconvolution to the moderate-growth spectrum over the entire range of n in which sufficient mass resolution is maintained (typically $n \leq 100$). From the analysis we extract the hydrogenation fraction, x_h , and the fractional abundance for each m , g_m .

One of the more dramatic effects, discussed qualitatively above, that we observe in the carbonaceous cluster distributions is the tendency for the even clusters above $n=40$ to appear as bare C_n while the odd clusters are hydrogenated. This effect is shown vividly in Fig. 3 in which we plot the hydrogenation fraction, x_h , versus cluster size, n , for the moderate-growth experiment. At low n both odd and even clusters show hydrogenation fractions that are high, 75-90%. At about $n=40$ there is a sharp drop in x_h for the even clusters while the hydrogenation fraction for the odd clusters stays high, never dropping much below 80%. The hydrogenation fraction is lowest for the even clusters in the $n=50-70$ range with a sharp minimum at $n=60$. The dramatic odd/even alternation near $n=60$ is shown quite nicely in the mass spectrum (Fig. 2); only 34% of the $n=60$ peak corresponds to $C_{60}H_m$ while 85% of the neighboring $n=61$ peak is due to hydrogenated species. Above $n=70$ the hydrogenation fraction gradually increases for even n and decreases for odd n , with the two curves apparently heading toward a common asymptote. This trend cannot be confirmed in this data because of the loss of mass resolution at $n > 100$.

We can quantify the tendency for even C_nH_m to appear with $m=2$ by examining the ratio of the fractional abundances for $m=2$ and $m=1$, g_2/g_1 . Fig. 3 displays a plot of g_2/g_1 versus n for the moderate-growth data. For the odd clusters this ratio stays constant at or near unity until around $n=70$. By contrast, g_2/g_1 is much larger for the even clusters until it drops quickly near $n=40$ so that for $n \geq 46$ the ratio is nearly identical for both odd and even clusters. This data demonstrates that with small amounts of hydrogen present in the source clusters as large as $n=44$ have a decided preference to appear as C_nH_2 ; odd clusters show no such preference. Near $n=60$, both even and odd clusters show a hydrogenation distribution that decreases monotonically with m and thus $g_2/g_1 < 1$. As n increases above about 70, the distributions widen and develop maxima at $m > 1$ so that the ratio g_2/g_1 gradually rises to values larger than unity.

DISCUSSION AND CONCLUSIONS

The mass spectra of C_nH_m ions for $8 \leq n \leq 20$, produced by multiphoton ionization of neutrals made by addition of various reactants to the carrier gas, have been discussed by Heath et al.¹³ They also observe the tendency for even clusters to form C_nH_2 species while the odd numbered clusters generally are found to have no distinctive hydrogenation pattern. The formation of C_nH_2 species is a strong signature of linear polyacetylenes of the form $H-C \equiv C-(C \equiv C)_m C \equiv C-H$. Heath et al. postulate that these form by the addition of two hydrogens to the terminal carbons of linear carbon chains that are triplet diradicals, $\cdot C \equiv C-(C \equiv C)_m C \equiv C \cdot$. Our data extends the results of Heath et al. to larger clusters. Interestingly, we observe a preference for C_nH_2 formation for even clusters up to $n=44$. This preference demonstrates that at least some of the C_nH_m species formed in our experiments are very long polyacetylenes. For $n \geq 10$ theoretical calculations for bare carbon clusters agree that monocyclic rings are more stable than linear chains. However, for reasons we now explore, it seems highly unlikely that long polyacetylenes are formed by hydrogenation of existing monocyclic rings.

In this type of experiment, where H_2 is added to the carrier gas upstream of the laser-induced plasma, we interpret the results in terms of a modification of the cluster growth that occurs without the reactant gas. The most important hydrogenation reactions are probably facile radical-radical reactions, i.e. reactions between H atoms and carbon or carbonaceous radicals. The results of Heath et al. support the assertion that H-atom reactions are important; they observe similar C_nH_m products for a variety of hydrogen-containing reactants.⁸ Under our experimental conditions the carbon density in the vaporization plume is in great excess of the H-atom concentration and carbon-cluster growth via reactions with small growth species (C , C_2 , and C_3) will proceed largely as if there was no reactant gas. The important difference is that hydrogen atom attack on a radical center might now render a cluster relatively inert with respect to further growth or hydrogenation. For even clusters with less than about 44 atoms this is observed as the formation of long polyacetylenes, the first non-radical species that can be formed

for a linear geometry. It is important to note that H-atom attack on a radical center might occur at any point in the cluster growth, not just at the end. For example, a linear C_{10} might be terminated at one end but continue to grow via carbon addition at the other, reactive end until it also encounters an H atom and is terminated.

The same picture of the modification of cluster (and ultimately particle) growth can be used to interpret our results for the larger carbonaceous clusters ($n \geq 40$). The results of our hydrogenation analysis of the data taken under moderate-growth conditions show dramatically the change in nature of the carbon and carbonaceous clusters near $n=40$. The plots of hydrogenation fraction and the ratio g_2/g_1 versus cluster size (Fig. 3) are particularly vivid in this regard. This pronounced change in behavior must be associated with a global change in geometric structure. Near $n=40$ the evidence for linear polyacetylenes disappears and the even clusters become inert relative to their odd neighbors. Clearly, even-numbered can adopt structures that do not have reactive, radical centers, i.e. closed shell fullerenes. By contrast, the odd clusters always appear hydrogenated, since they can only eliminate dangling bonds by hydrogenation.

As with the smaller clusters, the addition of hydrogen to the source in our experiments produces a relatively small perturbation in the overall growth of clusters and particles. One possible effect is that the H atoms in the cluster-growth region might decrease the likelihood of shell closure by tying up the radical sites at the edges of spiraling shells. However, the addition of hydrogen always accentuates the appearance of the fullerenes through the preferential hydrogenation of the neighboring odd clusters. This effect is especially pronounced in the low-growth spectra. On the basis of the low-growth C_n distribution alone, one might infer that both even and odd clusters are unclosed, reactive isomers, i.e. the even clusters have not yet found their way to closure. Yet, the addition of hydrogen under low-growth conditions clearly shows that some of the even clusters have already closed and become unreactive.

The implication of these results is that cluster growth and cluster hydrogenation are at least partially separable processes, with growth preceding hydrogenation. As noted above, it is dangerous to interpret our experiments entirely in this manner since hydrogen is present at all times in the course of cluster growth. However, such behavior can be rationalized both on fluid dynamic and thermodynamic grounds. Large clusters, and even particles, grow rapidly in the vaporization plume where the concentration of growth species in the carbon vapor is high relative to the hydrogen reactant. Significant hydrogenation may not take place until the vaporization plume is mixed by turbulence with the reactant/carrier gas mixture at points downstream. Also, in the high-temperature vapor plume the graphitic, spiraling shells are thermodynamically favored over their hydrogenated analogs. As the temperature drops during the flow through the source, irreversible hydrogenation of reactive sites can produce carbonaceous clusters. The even clusters can adopt closed structures under high-temperature pyrolytic conditions and thus become inert to subsequent hydrogenation at lower temperatures. By increasing the carrier gas density to our moderate-growth conditions, we drive the condensation process harder by increasing the carbon density in the high-temperature region, thereby allowing more even clusters to become fullerenes. Addition of small amounts of hydrogen under these conditions effectively "titrates" the odd clusters by hydrogenation but the unreactive even clusters emerge largely unscathed (see Fig. 2).

The conditions in our experiments are intentionally adjusted in order to avoid extensive hydrogenation. The relatively small amount of hydrogenation is thus insufficient to tie up all the reactive sites in a growing cluster and substantially slow further growth toward particles. The C/H ratio for the C_nH_m species that we produce in the moderate-growth experiment increases monotonically from ~ 6 at $n=20$ to ~ 18 at $n=100$. These values are much higher than what one would expect for spiraling shells whose reactive edges were completely saturated with hydrogens. As an upper bound on the C/H ratio of such species, consider the series of D_{6h} polycyclic aromatics of the form $C_{6j}H_{6j}$, i.e. C_6H_6 , $C_{24}H_{24}$, $C_{54}H_{54}$, $C_{96}H_{96}$, etc. The C/H ratio in these planar species is simply j ; the C/H ratio is 3 at $n=54$ and 4 at $n=96$. Generally, a partially closed shell will have fewer possibilities for C-H bonds than these species. A reasonable estimate might be a shell with half as many reactive sites; this gives a C/H ratio of 6-8 for $n=54-96$. We observe a C/H ratio of 15-20 in this size range in our moderate growth

experiment. This indicates that the hydrogenation distributions are still in the kinetically limited regime and do not represent saturation of all reactive sites. Finally, we note that our carbonaceous clusters are more carbon-rich than soot particles formed in combustion processes. Typically, nascent soot particles have a C/H ratio of 2-3 that may increase to 8-10 as the soot dehydrogenates at later stages in the flame.¹⁰

Our results, in which we study the formation of carbon and carbonaceous clusters in a laser-vaporization source with controlled addition of hydrogen, are quite similar to those obtained in a variety of other *in vacuo* laser vaporization studies¹⁻³ and in the flame studies of Homann et al.^{4,5} In all these cases, the large, even carbon clusters appear as the dominant mass spectral feature under conditions where there are substantial quantities of elements, especially hydrogen, other than carbon in the growth region. In our controlled hydrogenation studies we create conditions in which the neighboring odd clusters form a hydrocarbon background against which the fullerenes appear. We suspect that in some of the other vaporization studies and flame investigations the fullerenes stand out from a similar, unresolved hydrocarbon background, although the hydrogenation may be more extensive and thus spread the cluster distribution over a wider mass range. The idea that rapid carbon-cluster growth, and occasional fullerene shell closure, occurs in high-temperature regions where hydrogenation, or oxidation, is not favored must also apply to these environments. In the laser vaporization experiments, the high-temperature region is the laser-induced, high density plasma formed above the substrate, whether it be soot³ or various polymers.² In the flame studies, the fullerenes are found in the region where the temperature is near its maximum ($T \sim 2100$ K) and soot particles first begin to form.^{4,5} The exciting and unanswered question in these experiments is whether the fullerenes are created during soot formation, as proposed by Smalley and Kroto, or as the result of vaporization from the surface of a soot particle, as hypothesized by Homann et al.⁵

One of the great difficulties in elucidating the mechanism of soot inception is that the species one observes in a sooting flame, whether they be polycyclic aromatics or fullerenes, are the by-products of the process. The keys to any chemical mechanism are to be found in the radical species that control the kinetic pathway. Unfortunately in the case of soot formation, these radicals wind up buried in the soot particles; the manner in which they arrived there is but a distant memory. Analysis of the particles, while informative, cannot provide the data necessary to differentiate between hypothetical formation pathways.

In the future, we shall investigate the role of large carbonaceous clusters in soot inception and growth by concentrating on reaction studies of the reactive clusters. These may be the odd clusters, which can never completely close, or the reactive isomers of the even clusters. The cluster beam source provides an ideal forum for studies of reactive intermediates because these species can be frozen out in the free jet expansion. We shall perform more studies, such as those presented here, in which reactants are added upstream of the vaporization. Of particular interest is the formation of carbonaceous clusters under conditions that emulate those in a sooting flame, i.e. oxidative, not just pyrolytic. In addition, we shall pursue more controlled chemical reactions using the fast-flow reactor techniques that have been used so successfully in the study of metal cluster chemistry. Zhang et al. have performed some initial work in this area on the large carbon clusters.⁸ However, their study was aimed principally at the unique, unreactive nature of the fullerenes; the products of reactions with odd clusters were observed only as unresolved background. We intend to use the high resolution of the reflectron to sort out the products of reactions such as $C_nH_m + C_2H_2$, which represents a model for the growth of a soot particle through the addition of acetylene. Again, the emphasis will be on arresting the growth process in order to examine clusters that are reactive intermediates and not on the stable by-products, such as the fullerenes.

References

1. D. N. Lineman, K. V. Somayajula, A. G. Sharkey, and D. M. Hercules, *J. Phys. Chem.* **93** (1989) 5025.
2. W. R. Creasy and J. T. Brenna, *J. Chem. Phys.* **92** (1990) 2269; W. R. Creasy and J. T. Brenna, *Chem. Phys.* **126** (1988) 453.
3. H. Y. So and C. L. Wilkins, *J. Phys. Chem.* **93** (1989) 1184.

4. Ph. Gerhardt, S. Löffler, and K. H. Homann, *Chem. Phys. Lett.* **137**, 306 (1987).
5. Ph. Gerhardt, S. Löffler, and K. H. Homann, *Twenty-Second Symposium (International) on Combustion*, p. 395 (The Combustion Institute, 1989).
6. H. W. Kroto, *Nature* **329**, 529 (1987).
7. H. W. Kroto and K. McKay, *Nature* **331**, 328 (1988).
8. Q. L. Zhang, S. C. O'Brien, J. R. Heath, Y. Liu, R. F. Curl, H. W. Kroto, and R. E. Smalley, *J. Phys. Chem.* **90**, 525 (1986).
9. R. M. Baum, "Ideas on Soot Formation Spark Controversy," *Chem. and Eng. News*, February 5, 1990, p. 30.
10. S. J. Harris and A. M. Weiner, *Ann. Rev. Phys. Chem.* **36**, 31 (1985).
11. K. H. Homann, *Twentieth Symposium (International) on Combustion*, p. 857 (The Combustion Institute, 1984).
12. H. GG. Wagner, *Seventeenth Symposium (International) on Combustion*, p. 3 (The Combustion Institute, 1979).
13. J. R. Heath, Q. Zhang, S. C. O'Brien, R. F. Curl, H. W. Kroto, and R. E. Smalley, *J. Am. Chem. Soc.* **109**, 359 (1987).
14. E. A. Rohlfing, *J. Chem. Phys.* **93**, 7851 (1990).

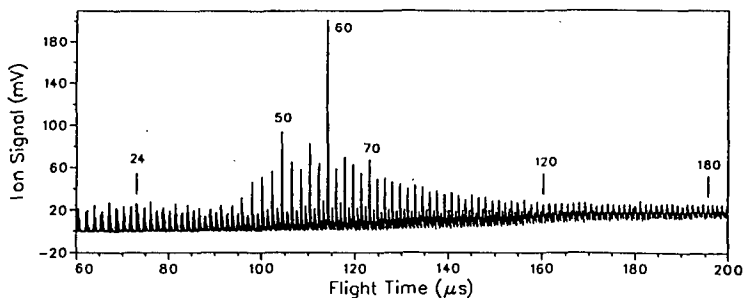


FIG 1. Reflectron TOF mass spectrum of carbonaceous clusters, C_nH_m , produced with a 0.5% H_2/He mixture as the carrier gas under moderate-growth conditions in the cluster source.

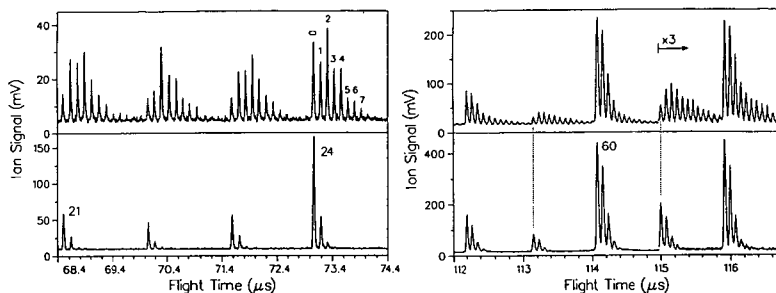


FIG. 2. Close-up views ($n=21-24$ and $n=58-62$) of the C_n and $C_n H_m$ mass spectra taken under moderate-growth conditions. Top panels: spectra of C_n taken with He carrier gas; bottom panels: spectra of $C_n H_m$ taken with 0.5% H_2 /He carrier gas.

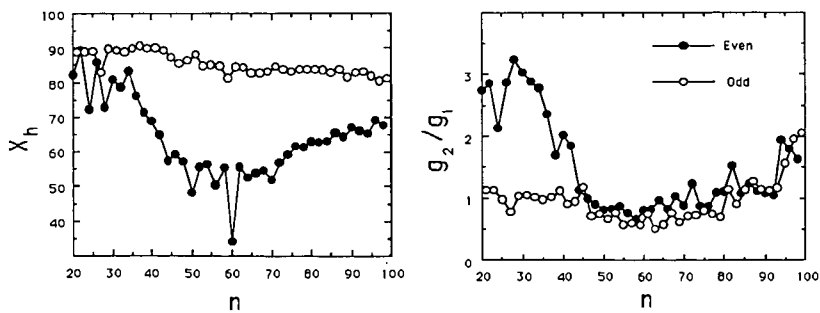


FIG. 3. Results of hydrogenation analysis for moderate-growth $C_n H_m$ mass spectrum (Fig. 1) as a function of cluster size, n . Left: the fraction of hydrogenated species. Right: the ratio of fractional abundances of for $m=1$ and $m=2$.